

Cone Beam Computed Tomography: Craniofacial and Airway Analysis

David C. Hatcher, DDS, MSc^{a,b,c,*}

KEYWORDS

- Cone beam CT (CBCT) • Volumetric imaging
- Degenerative joint disease • TMJ • Airway
- Retroglossal • Retropalatal • Facial growth

Imaging plays a role in the anatomic assessment of the airway and adjacent structures. Obstructive sleep-disordered breathing (OSDB) is not diagnosed with imaging, but imaging can identify patients with airways who are at risk for obstruction and other anatomic characteristics that may contribute to OSDB. The airway extending from the tip of the nose to the superior end of the trachea can be visualized on conventional computed tomography (CT) and cone beam CT (CBCT) scans. Because these scans also include the jaws, teeth, cranial base, spine, and facial soft tissues, there is an opportunity to evaluate the functional and developmental relationships between these structures. The skeletal support for airway is provided by the cranial base (superiorly), spine (posteriorly), nasal septum (anterosuperiorly), jaws, and hyoid bone (anteriorly). The airway valves include the soft palate, tongue, and epiglottis (**Fig. 1**). Airway obstructions or encroachments are of interest because they increase airway resistance that may contribute to OSDB; therefore, visualization and calculation of the airway dimensions are important. Common airway encroachments include turbinates, adenoids, long soft palate, large tongue, and pharyngeal and lingual tonsils. Less common airway encroachments include polyps and tumors.

This article discusses the use of 3-dimensional (3D) imaging (CBCT) to evaluate the airway and

selected regional anatomic variables that may contribute to OSDB. Optimal treatment outcomes begin with a complete and accurate diagnosis. Imaging may assist in delineating attributes that contribute to OSDB in patients who do not have a phenotype (such as high body mass index) that is routinely associated with OSDB.

CBCT AND IMAGE ANALYSIS

Technological advances in computing power, sensor technology, and reconstruction algorithms have merged and resulted in the introduction of a CBCT (also known as volumetric imaging). Volumetric imaging is synonymous with 3D imaging because the information has depth in addition to length and width. The 3D imaging domain includes radiograph (CT and CBCT) and magnetic resonance imaging technologies. The 2 principal differences that distinguish CBCT from traditional CT are the type of imaging source-detector complex and the method of data acquisition. The radiograph source for CT is a high-photon, output rotating anode generator, whereas for CBCT it can be a low-energy fixed anode tube similar to that used in dental panoramic machines. CT uses a fan-shaped x-ray beam from its source to acquire images and records data on solid-state image detectors that are arranged in a 360° array

^a University of Southern Nevada, 11 Sunset Way, Henderson, NV 89014, USA

^b Arthur A. Dugoni School of Dentistry, 2155 Webster Street, San Francisco, CA 94115, USA

^c Private Practice, Diagnostic Digital Imaging, 99 Scripps Drive, #101, Sacramento, CA 95825, USA

* University of Southern Nevada, 11 Sunset Way, Henderson, NV 89014.

E-mail address: David@ddicenters.com

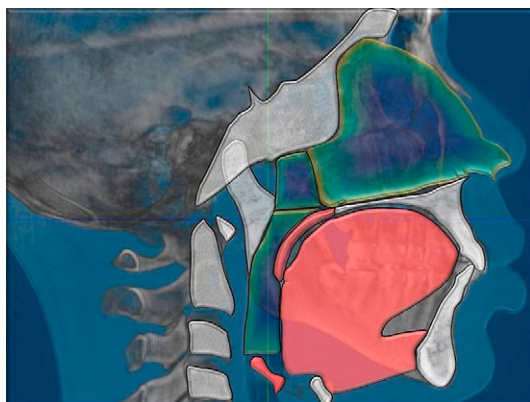


Fig. 1. Airway zones that are visible using CBCT (*blue and green*). These zones extend from the nasal tip to the epiglottis and are divided in the nasal, nasopharyngeal, and oral airways. The airway is supported posteriorly by the spine; superiorly by the cranial base; and anteriorly by the maxilla, mandible, and hyoid (*white*). The mobile elements associated with the airway include the tongue, soft palate, and epiglottis (*red*).

around the patient. CBCT technology uses a cone-shaped x-ray beam with a special image intensifier and a solid-state sensor or an amorphous silicon plate for capturing the image.

Conventional medical CT devices image patients in a series of axial plane slices that are captured either as individual stacked slices or using a continuous spiral motion over the axial plane. Conversely, CBCT presently uses one rotation sweep of the patient similar to that used for panoramic radiography. Image data can be collected for either a complete dental/maxillofacial volume or a limited regional area of interest. Scan times for these vary from 8 to 40 seconds for the complete volume. CBCT has a significantly lower radiation burden than a comparable scan using a conventional CT. CBCT has a favorable risk/benefit ratio for many craniofacial applications, including imaging of the airway and associated craniofacial structures.

ANATOMIC ACCURACY

An ideal imaging goal is to accurately represent the anatomy as it exists in nature, that is, the anatomic truth. The projection geometry associated with 2D techniques does not produce accurate anatomic images. 3D digital techniques using back projection algorithms create the opportunity to produce anatomically accurate images.

Current 3D imaging techniques allow an anatomically accurate capture of the surface and subsurface structures.¹⁻⁴ One measure of image

quality is the ability to detect small anatomic features. The variables that have significant influence on the quality of a CBCT include voxel size (smallest element in a 3D digital image), dynamic range (number of gray levels), signal, and noise. In general, the best quality image is composed of small voxels, large number of gray levels, high signal, and low noise. CBCT voxels are isotropic (equal size in all dimensions x, y, and z) and range in size from 0.1 to 0.4 mm. The captured field of view (FOV) can be scaled to match the regions of interest (ROIs). The ROI can include the entire craniofacial region or a selected subsection of the craniofacial anatomy. The display of the captured FOV or subset of image data can be viewed from any angle using various display techniques (**Fig. 2**). For example, the entire craniofacial skeleton may be captured using a CBCT scan, but using software tools, an ROI (such as the airway) may be selected, displayed, and analyzed. Several software companies have developed application-specific display and analysis software that result in the measurement (linear, area, volume, angular) of segmented and integrated anatomic structures. Of particular interest is the metric analysis of the airway and the adjacent structures. Specialized software for metric analysis of the airway has been calibrated using orthogonal and oblique airway phantoms, and has been validated for accuracy and precision.^{2,3} The convergence of CBCT with the application software is very beneficial in understanding and diagnosing OSDB and its relationship to craniofacial anatomy.

FACIAL GROWTH AND THE AIRWAY

Alterations from the normal pattern of nasal respiration occurring during active growth can affect the development of the craniofacial skeleton in humans and experimental animals.⁵⁻⁸ Severely reduced nasal airflow may induce compensations that include an inferior mandibular rest position, parting of the lips, increased interocclusal space, lower or more forward tongue position, lower positioning of the hyoid bone, a modal shift from nasal breathing to mouth breathing, anterior extension of the head and neck, increased anterior face height, increase in the mandibular and occlusal plane angles, narrow alar base, narrow maxillary arch, high palatal vault, posterior crossbite, class II occlusion, and clockwise facial growth pattern. These compilations of craniofacial and occlusal traits produce a facial phenotype that has been cited in the orthodontic literature as “adenoidal facies,” thus ascribing an etiology and expressing a bias that hypertrophic adenoidal tissues are the cause of an obtunded nasal airflow that results in

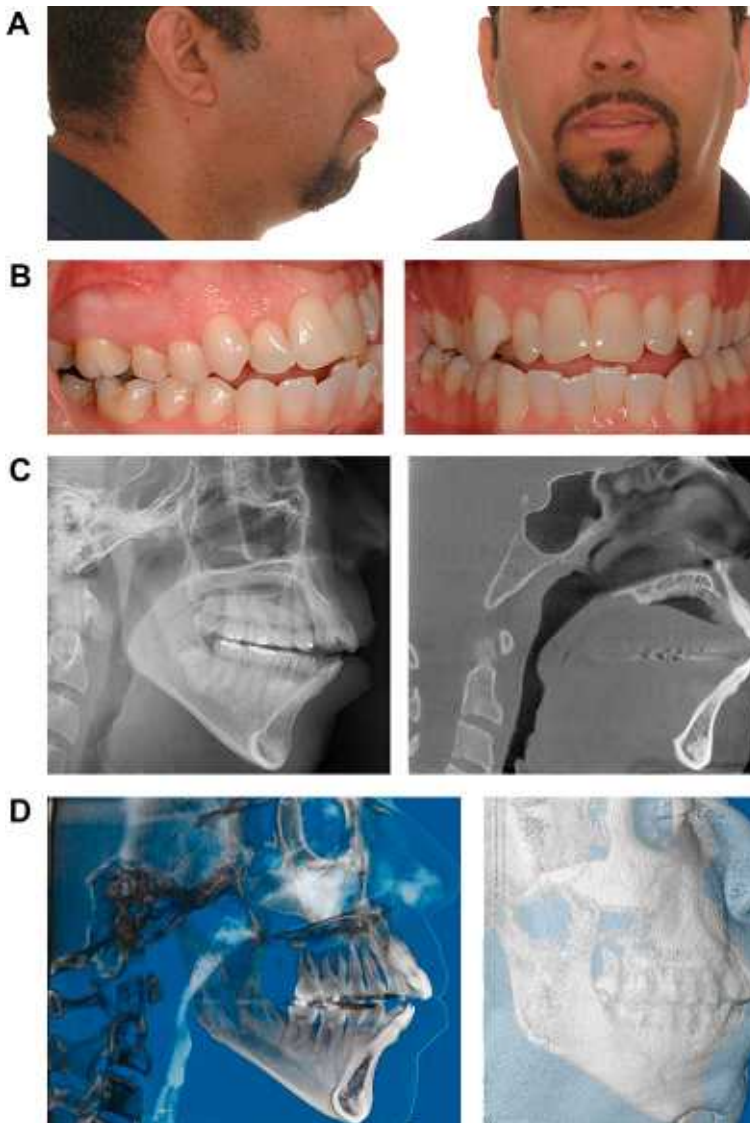


Fig. 2. Craniofacial and airway visualization. Various CBCT and patient visualization options. (A, B) Convex facial profile, narrow maxilla, anterior open bite, and forward head and neck posture. (C) Midsagittal airway (*right image*) and a standard cephalometric image generated from the CBCT volume using specialized software. (D) Volume-rendered and shaded surface display image of the head and neck skeleton along with the airway-skin boundaries. (E) Analysis of the airway. The midsagittal airway view is mapped (*left image*), and a series of cross-sectional areas (CSAs) of the mapped regions are generated (*right image*). The CSA and distance measurements are calculated and displayed for each of the cross-sectional intervals. The smallest cross-sectional area was identified to be 38.94 mm². (F) A reconstructed panoramic projection. The data volume can be reconstructed in any user-defined orthogonal, oblique, or curved plane to match the clinical investigation objective. Note the small condyles and forward posture of the mandible.

a specific pattern of craniofacial deformation. However, this facial phenotype may also occur secondary to aberrant mandibular growth. The end result in several craniofacial growth scenarios may be associated with alterations in airway dimensions, airway resistance, and functional airway patency, but the cause-and-effect

relationships need to be considered. For example, does an anatomic reduction in airway function cause the craniofacial compensations or does abnormal craniofacial growth result in compromised airway function? The anteroposterior dimensions of the airway have been shown to have a proportional relationship to jaw growth

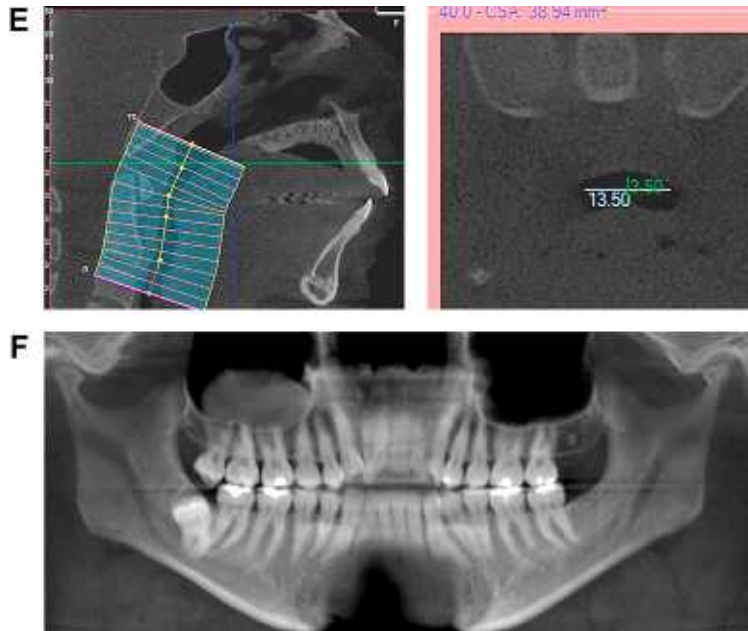


Fig. 2. (continued)

and facial growth pattern.⁹ The airway is largest when there is normal mandibular and maxillary growth and when facial growth pattern occurs with a counter-clockwise rotation. Conversely, the airway is smaller with deficient maxillary and mandibular growth and when there is a clockwise facial growth pattern. Because mandibular growth has been linked to condylar growth and degenerative joint disease (DJD, also known as osteoarthritis) affects condylar growth, it is reasonable to postulate that a developmental onset of DJD may limit airway dimensions (**Figs. 3 and 4**).

Current 3D imaging techniques available for routine imaging provide the opportunity to use a “systems approach” to visualize and evaluate the functional and developmental relationships between proximal craniofacial regions. It has been reported that a developmental insult to the temporomandibular joints (TMJs) may have a regional effect on the growth of the ipsilateral side of the face, including the mandible, maxilla, and base of the skull.^{10–18} Similarly, there is a direct relationship between jaw growth and airway development.⁹ The notion that there are functional and growth relationships between adjacent anatomic regions creates the desire for a robust method to visualize and analyze them.

MANDIBULAR GROWTH

The mandible forms by using a combination of endochondral and intramembranous processes

of bone formation. The condyles do not control growth of the entire mandible, but condylar growth contributes to the process of mandibular growth, primarily the condylar processes and rami, and secondarily the body and alveolar ridges. Mesenchymal cell differentiation into articular cartilage followed by endochondral ossification contributes to the condylar growth. There are several mandibular growth sites (growth fields), including the condyles, alveolar process, rami, body, and coronoid process. These growth sites have genetic potential for growth through mesenchymal cell differentiation and cell division, but the growth can be modulated through external or environmental (epigenetic) factors. These external factors include neighboring growth sites, hormones, tissue stress and strain, and tissue damage. The craniofacial complex generally grows in harmony. Changes occurring in one area of the craniofacial complex induce a response in the adjacent areas. A model proposed by Petrovic and coworkers^{12,13} suggests that distant craniofacial changes (such as maxillary growth) are transformed into local (mandibular) growth signals by a complex interplay of muscle adaptation, neural input, connective tissue response, blood supply, biochemical growth activation, and suppression. Condylar fibrocartilage, during growth, is responsive to growth stimuli from various systemic and local influences. Ideally, condylar growth is modulated to keep pace with facial growth. Fibrocartilage in the adult condyle

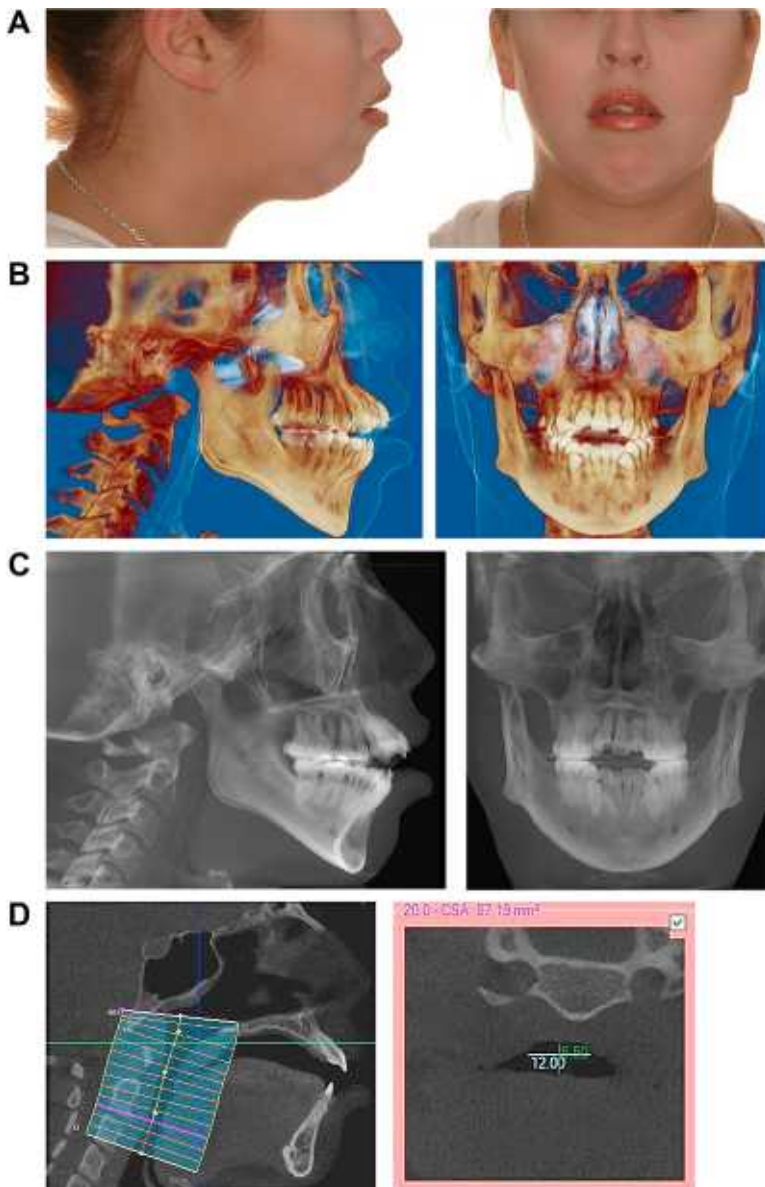


Fig. 3. Temporomandibular joint (TMJ), facial growth, and airway. A craniofacial phenotype that occurs after a developmental onset of TMJ DJD. The DJD limited or arrested the development of the condyles, and this resulted in reduced mandibular growth along with other craniofacial compensations (*F*). The condyles were located in the anteroinferior regions of their fossa when in habitual occlusion (*F*). Note the convex facial profile (*A–C*), the anterior open bite (*B–D*, *E*, *F*), and the forward head and neck posture. The mediolateral development of the maxilla and mandible was reduced (*B*, *C*, *E*), and the tongue was postured down and away from the depth of the palate. There was diffuse narrowing of the airway with the smallest cross-sectional area measuring 87.19 mm². The forward posture of the mandible may be a compensation to improve airway patency. Selective muscle recruitment is required to resist the clockwise rotation of the mandible and maintain airway patency.

has an adaptive function to maintain the mandible in its functional role. Reduced adaptive capacity of the fibrocartilage (such as DJD) during growth and development has been shown to limit growth of the ipsilateral half of the mandible. DJD in adulthood that results in significant hard tissue loss may be associated with a change in mandibular

posture, occlusion, and condyle/fossa spatial relationships.

DEGENERATIVE JOINT DISEASE

DJD (also known as degenerative arthritis, degenerative arthrosis, osteoarthritis, and osteoarthritis)



Fig. 3. (continued)

affects all joints, including the TMJ. There are several factors that can initiate the pathologic and imaging features associated with DJD. These factors create a situation whereby the articular structures can no longer resist the applied forces to the joint. DJD involves the destruction of the hard and soft articular tissues, and occurs when the remodeling capacity of those tissues has been exceeded by the functional demands. Therefore, scenarios that modulate and increase joint loads or diminish the strength or adaptive capacity of the articular tissues are of interest in discovering the pathogenesis of TMJ DJD. The understanding of DJD has significantly evolved during the past 30 years. Until recently, DJD of the TMJ was considered a wear and tear phenomenon that occurred in individuals older than 40 years, as observed in other synovial joints. However, recent investigations and clinical observations have discovered significant differences in the occurrence and behavior of TMJ DJD in comparison with other joints. TMJ DJD has been recognized to have a predilection for women and can be identified at all ages after puberty, and is not limited to individuals older than 40 years. It has been suggested that sex hormones and hormone receptors may play a role in the early age onset and sex predilection of this phenomenon. DJD onset and the associated complaints in women occur from puberty through menopause. The TMJ is a diarthrodial joint like other synovial joints; however, the expression of DJD differs from other joints. Key distinctions between the TMJ anatomy and other synovial joints include the predominance of

fibrocartilage in lieu of hyaline cartilage and motion mechanics that include rotation and translation. The TMJ is a loaded joint, and the joint loads or stress concentrations (force/area) may be equal to other load-bearing joints.¹⁸ The functional movement of the condyle over the disk creates a contact force (F) applied in a direction ($\cos \theta$) over a distance (d) during a specific time (t) interval. The disk/condyle interactions can be expressed in terms of work (W) or power (P); $W = F \times d \times \cos \theta$ and $P = W/t$.^{19–22} Investigators are currently examining the mechanobiology or single-cell biomechanics, that is, how physical forces influence biologic processes in the TMJ.^{23–26} Single-cell biomechanics depend on their material properties relative to the surrounding matrix. The TMJ disk cells are a heterogeneous mixture of fibroblasts and fibrochondrocytes. The TMJ disk is a fibrocartilaginous tissue, but it is not a homogeneous tissue. The disk is composed mostly of collagen (type I), proteoglycans (glycosaminoglycan chains that are primarily chondroitin sulfate and dermatan sulfate), and water. The distribution and arrangement of the disk components are not uniform. This disk has been divided into 3 areas or zones: the anterior band, the intermediate zone, and the posterior band. These zones, like anatomic regions, create material property differences, and therefore the single-cell biomechanics between these zones may vary. The anatomic variations between the zones ideally reflect a structural relationship to the functional demands in terms of work and power. The work imparted on the tissues (cells) initiates a mechanotransduction pathway (mechanism by

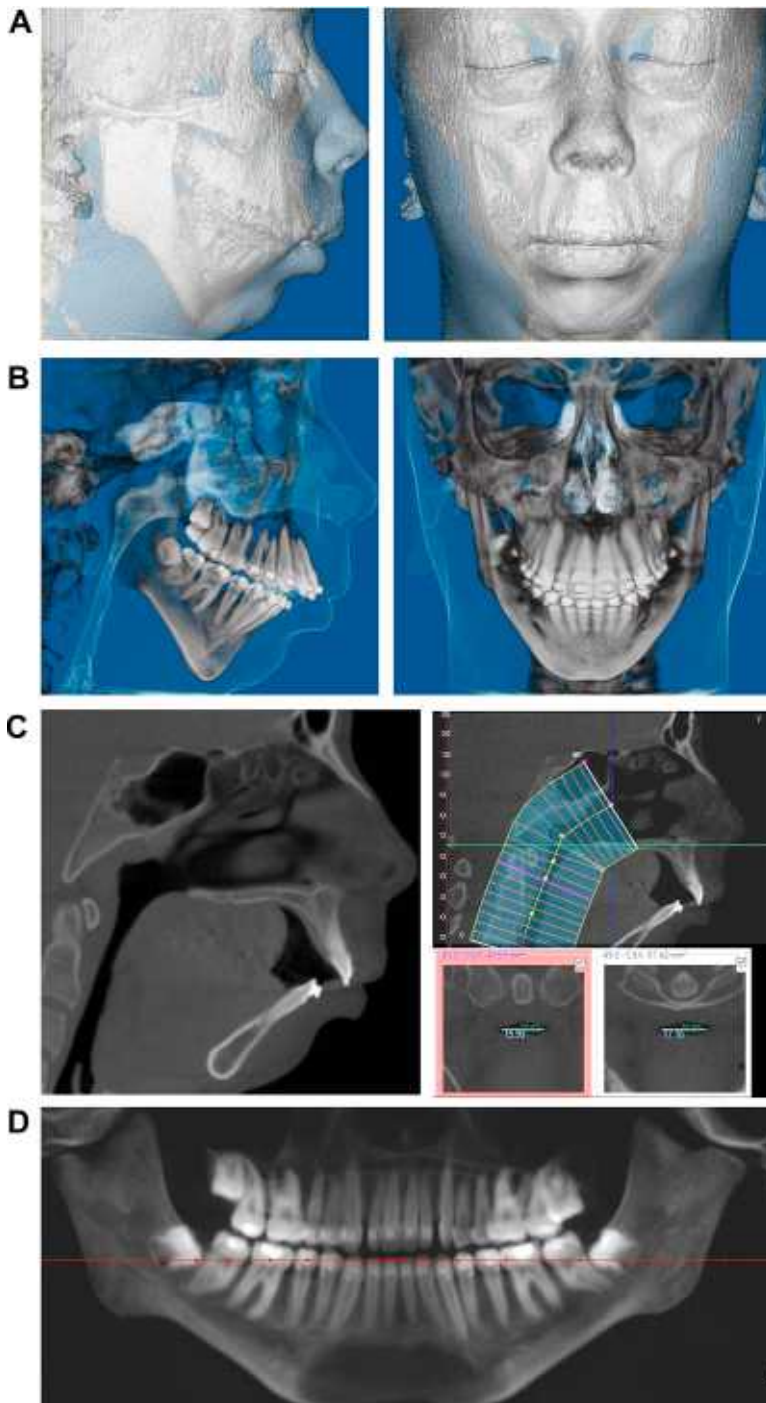


Fig. 4. (A–D) TMJ, facial growth, and airway. A craniofacial phenotype that occurs after a developmental onset of TMJ juvenile rheumatoid arthritis (JRA). The regional compensations to the JRA were similar to those observed in Fig. 3 for DJD. There was a convex facial profile, clockwise facial growth pattern, steep mandibular and occlusal planes, obtuse gonial angles, small mediolateral jaw dimensions, inferior positioning of hyoid bone, anterior open bite, and small airway. The airway dimensions were diffusely narrowed with the smallest cross-sectional area measuring 49.59 mm^2 .

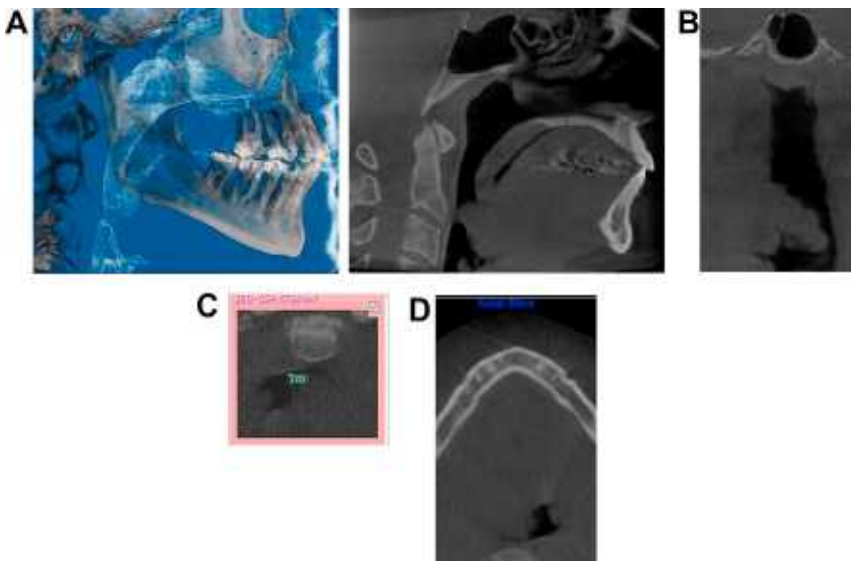


Fig. 5. Tumor; airway encroachment. (A) A soft tissue density extending from the tongue base region and encroaching on the airway space. (B–D) Soft tissue density extending from the right lateral wall of the oral pharynx. This soft tissue encroachment was determined to be a squamous cell carcinoma that had reduced the cross-sectional area to 87.93 mm².

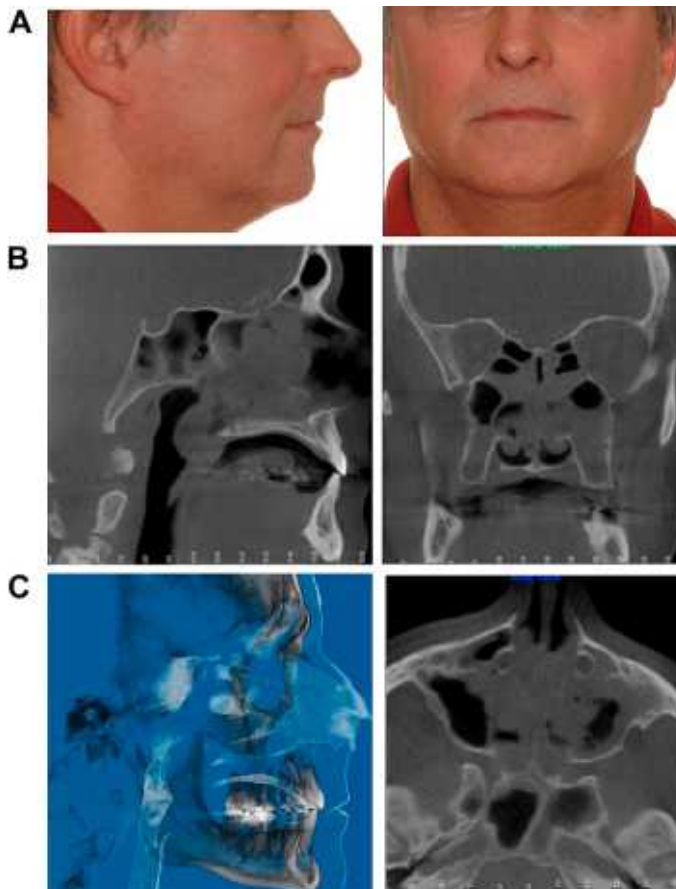


Fig. 6. Inflammatory disease; upper airway encroachment. A patient with severe rhinosinusitis (A). The ostiomeatal units and the nasal fosse were not patent. A polyp was extending into the nasopharynx (B, left image). A discontinuity of the airway spaces of the nose and the oral pharynx (C, left image) (air shown as white).

which cells convert a mechanical stimulus into a chemical activity) that results in gene expression. Gene expression initiates several pathways to produce (1) extracellular matrix proteins, (2) matrix metalloproteinases, (3) proinflammatory cytokines, or (4) apoptosis regulators. The extracellular matrix protein synthesis creates extracellular matrix and tissue regeneration. The production of matrix metalloproteinases and proinflammatory cytokines results in extracellular matrix degradation. Extracellular matrix degradation and apoptosis are pathways that can result in DJD. The variations in mechanotransduction pathways may be related to the tissue anatomy, tissue quality, and power (work/time). Several variables affect work, including peak forces, force vectors, velocity, and work cycles. The tissues' anatomy and quality will relate to the adaptive capacity of those tissues. Both mechanotransduction and signal transduction by hormones (β -estradiol, relaxin, progesterone) are currently being explored.^{27,28} In vivo testing on rabbits using disk explants has demonstrated that increased serum levels of relaxin, β -estradiol and relaxin, and β -estradiol result in the loss of glycosaminoglycans and collagen from

fibrocartilaginous sites (ie, TMJ and pubic symphysis) but not from hyaline cartilaginous sites. Relaxin and β -estradiol induced the matrix metalloproteinase expression of collagenase-1 and stromelysin-1. It was also shown that progesterone prevented the loss of matrix molecules. This hormone-induced, targeted matrix degradation may be the key to the understanding of why TMJ DJD is most commonly seen in women during their reproductive years. There is likely interplay between mechanotransduction and hormonal transduction of matrix degradation proteinases during the onset and progression of DJD.

DJD: IMAGING OBSERVATIONS

Current imaging modalities have revealed several stages associated with DJD that progress along a continuum from normal, failure, repair, and stability.¹⁸ It has been observed that soft tissue changes occur first, and this progresses to the involvement of hard tissues in a small percentage of individuals. It has been proposed that DJD progresses until the functional forces (work and

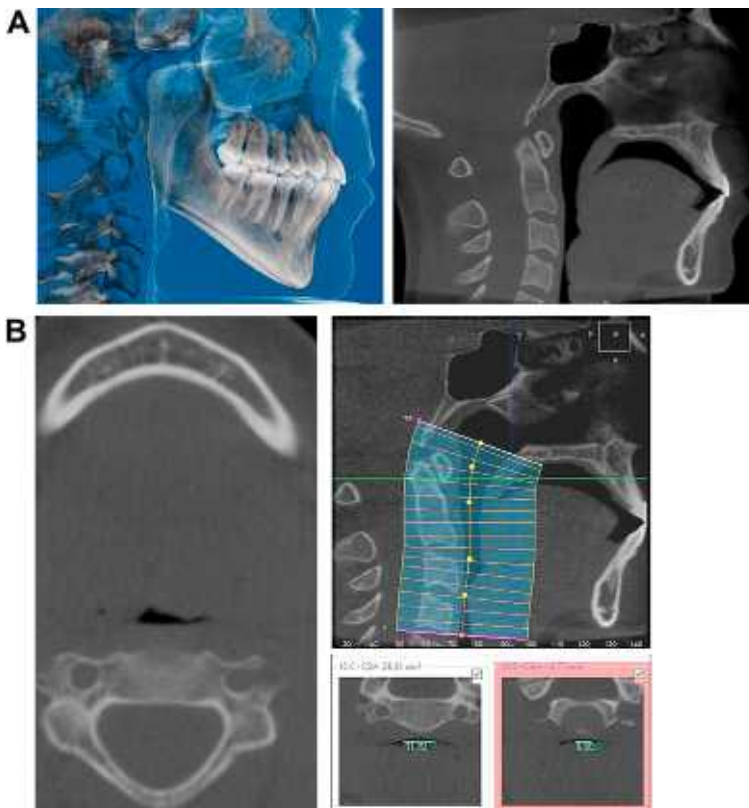


Fig. 7. Lingual tonsils; base of tongue encroachment. (A, B) The airway of a patient with large lingual tonsils. The airway at base of the tongue was calculated to be 13.77 mm².

power) are modulated by tissue changes to be within the adaptive capacity of targeted tissues.

AIRWAY

3D imaging is a very efficient method to inspect and identify diffuse narrowing (narrowing disturbed over a large distance) or focal narrowing (encroachments) of the airway. A reduction in

airway radius increases the airway resistance as described by Poiseuille's law ($R = 8nl/pr^4$) where R is resistance, n is viscosity, l is length, and r is radius. Airflow maintenance requires increased inspiration effort as the resistance to airflow increases as described by Ohm's law ($V = P_{\text{mouth}} - P_{\text{alveoli}}/R$) where V is flow, P is pressure, and R is resistance. The increased inspiration effort results in a greater differential pressure

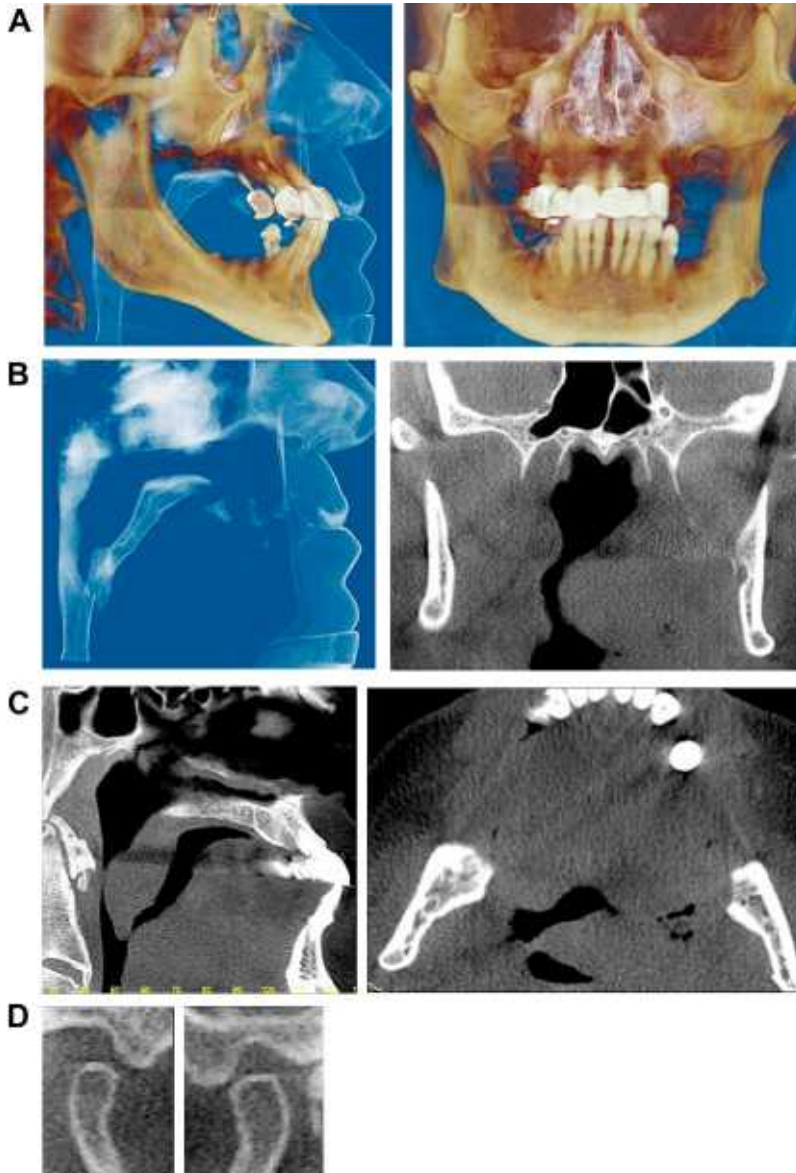


Fig. 8. (A–D) Tumor; upper airway encroachment. This individual was scanned using a CBCT and displayed using multiplanar sections and volume rendering. The condyles were in an acquired anteroinferior position within their fossa. A soft tissue mass was identified, extending from the left lateropharyngeal wall and extending into and enlarging the dimensions of the soft palate. This mass was determined to be a squamous cell carcinoma. The mass had reduced the airway dimensions, and the patient found it necessary to hold the jaw forward to maintain airway patency.

between the mouth and the alveoli. The airway, an elastic tube, is collapsible and is susceptible to the generation of a large pressure gradient between the lung alveoli and mouth. Mobility of the selected airway valves, such as the tongue, nares, soft palate, and epiglottis, may increase under the influence of increased respiratory pressure. Increased resistance in the airway requires a greater inspiratory pressure to maintain airflow predisposing to airway collapse.

Multivariate analysis shows both retroglossal ($P = .027$) and retropalatal spaces ($P = .0036$) to be predictive of respiratory disturbance index. Li and colleagues²⁹ have also demonstrated a relationship between the airway area and the likelihood of obstructive sleep apnea (OSA). There is a high probability of severe OSA if the airway area is less than 52 mm², an intermediate probability if the airway is between 52 to 110 mm², and a low probability if the airway is greater than 110 mm².^{30–32} Lowe and colleagues³⁰ demonstrated that most constrictions occur in the oropharynx with a mean airway volume of 13.89 ± 5.33 cm³. Barkdull and colleagues^{33,34} demonstrated a correlation between the retro-lingual cross-sectional airway and OSA when this area was less than 4% of the cross-sectional area of the cervicomandibular ring. Encroachments that increase resistance can occur anywhere along the length of the airway and include rhinitis, deviate septum, polyps, tonsils, adenoids, and tumors (see Fig. 4; Figs. 5–8).

SUMMARY

Incorporation of 3D imaging into daily practice will allow practitioners to readily evaluate and screen patients for phenotypes associated with OSDB. This is particularly important in the adolescent population where many already seek orthodontic treatment for dentofacial deformities associated with OSDB.

The introduction and availability of CBCT has created the opportunity to serially examine individuals and acquire accurate 3D anatomic information. The “systems approach” of observing and testing the interactions and influence that adjacent regions have on each other will be a key to the understanding of the biomechanical influences on craniofacial form and the role they play in OSDB.

REFERENCES

1. Stratemann S, Huang J, Makik K, et al. Comparison of cone beam computed tomography imaging with physical measures. *Dentomaxillofac Radiol* 2008; 37(2):80–93.
2. Schendel SA, Hatcher D. CBCT semiautomated 3D airway analysis. *J Oral Maxillofac Surg* 2010. [Epub ahead of print].
3. Aboudara C, Nielsen I, Huang JC, et al. Comparison of airway space with conventional lateral head films and 3-dimensional reconstruction from cone-beam computed tomography. *Am J Orthod Dentofacial Orthop* 2009;135(4):468–79.
4. Aboudara CA, Hatcher D, Neilsen IL, et al. A three-dimensional evaluation of the upper airway in adolescents. *Orthod Craniofac Res* 2003;6(Suppl 1):173–5.
5. Woodside D, Linder-Aronson S, Ludstrom A, et al. Mandibular and maxillary growth after changed mode of breathing. *Am J Orthod Dentofacial Orthop* 1991;100:1–18.
6. Yamada T, Tanne K, Miyamoto K, et al. Influences of nasal respiratory obstruction on craniofacial growth in young *Macaca fuscata* monkey. *Am J Orthod Dentofacial Orthop* 1997;11:38–43.
7. Solow B, Siersback-Nielsen S, Greve E. Airway adequacy, head posture, and craniofacial morphology. *Am J Orthod* 1984;86:214–23.
8. Vargervik K, Miller A, Chierici G, et al. Morphologic response to changes in neuromuscular patterns experimentally induced by altered modes of respiration. *Am J Orthod* 1984;85:115–24.
9. Stratemann S. 3D craniofacial imaging: airway and craniofacial morphology [Unpublished MSc thesis], Department of Growth and Development. University of California San Francisco; 2005.
10. Legrell PE, Isberg A. Mandibular length and midline asymmetry after experimentally induced temporomandibular joint disk displacement in rabbits. *Am J Orthod Dentofacial Orthop* 1999; 115(3):247–53.
11. Legrell PE, Isberg A. Mandibular height asymmetry following experimentally induced temporomandibular joint disk displacement in rabbits. *Oral Surg Oral Med Oral Pathol Oral Radiol Endod* 1998; 86(3):280–3.
12. Stutzmann JJ, Patrovic AG. Role of the lateral pterygoid muscle and menisco temporomandibular frenum in spontaneous growth of the mandible and in growth stimulated by the postural hyperpropulsor. *Am J Orthod Dentofac Orthop* 1990;97:381–92.
13. Petrovic AG. Heritage paper. Auxologic categorization and chronobiologic specific for the choice of appropriate orthodontic treatment. *Am J Orthod Dentofac Orthop* 1994;105(2):192–205.
14. Nebbe B, Major PW. Prevalence of TMJ disc displacement in a pre-orthodontic adolescent sample. *Angle Orthod* 2000;70(6):454–63.
15. Flores-Mir C, Akbarimaneh L, Nebbe B, et al. Longitudinal study on TMJ disk status and its effect on mandibular growth. *J Orthod* 2007;34(3):194–9.

16. Flores-Mir C, Nebbe B, Heo G, et al. Longitudinal study of temporomandibular joint disc status and craniofacial growth. *Am J Orthod Dentofacial Orthop* 2007;131(5):575–6.
17. Nebbe B, Major PW, Prasad N. Female adolescent facial pattern associated with TMJ disk displacement and reduction in disk length: part I. *Am J Orthod Dentofacial Orthop* 1999;116(2):168–76.
18. Hatcher DC, McEvoy SP, Mah RT, et al. Distribution of local and general stresses in the stomatognathic system. In: McNeill C, editor. *Science and practice of occlusion*. Chicago: Quintessence Publishing Co; 1997. p. 259–72.
19. Mah RT, McEvoy SP, Hatcher DC, et al. Engineering principles and modeling strategies. In: McNeill C, editor. *Science and practice of occlusion*. Chicago: Quintessence Publishing Co; 1997. p. 153–64.
20. Gallo LM, Chiaravolloti G, Iwaskai LR, et al. Mechanical work during stress field translation in the human TMJ. *J Dent Res* 2006;85(11):1006–10.
21. Nickel JC, Iwaskai LR, Beatty MW, et al. Static and dynamic loading effects on temporomandibular joint disc tractional forces. *J Dent Res* 2006;85(9):809–13.
22. Nickel JC, Iwaskai LR, Beatty MW, et al. Laboratory stresses and tractional forces on the TMJ disc surface. *J Dent Res* 2004;83(8):650–4.
23. Lammi M. Current perspective on cartilage and chondrocyte mechanobiology. *Biorheology* 2004; 41:593–6.
24. Turner CH. Biomechanical aspects of bone formation. In: Bronner F, Farach-Carson MC, editors. *Bone formation*. London: Springer Press; 2004. p. 79–105.
25. Carter DR, Beaupré GS, Wong M, et al. The mechanobiology of articular cartilage development and degeneration. *Clin Orthop Relat Res* 2004;(Suppl 427):S69–77.
26. Huang H, Kamm RD, Lee RT, et al. Cell mechanics and mechanotransduction: pathways, probes, and physiology. *Am J Physiol Cell Physiol* 2004;287: C1–C11.
27. Hashem G, Zhang Q, Hayami T, et al. Relaxin and beta-estradiol modulate targeted matrix degradation in specific synovial joint fibrocartilages: progesterone prevents matrix loss. *Arthritis Res Ther* 2006;8(4):R98.
28. Naqvi T, Duong T, Hashem G, et al. Relaxin's induction of metalloproteinases is associated with loss of collagen and glycosaminoglycans in synovial joint fibrocartilaginous explants. *Arthritis Res Ther* 2005; 7(1):R1–R11.
29. Li HY, Chen NH, Wang CR, et al. Use of 3-dimensional computed tomography scan to evaluate upper airway patency for patients undergoing sleep-disordered breathing surgery. *Otolaryngol Head Neck Surg* 2003;129:336–42.
30. Lowe AA, Gionhaku N, Takeuchi K, et al. Three-dimensional CT reconstructions of tongue and airway in adult subjects with obstructive sleep apnea. *Am J Orthod Dentofacial Orthop* 1986; 90(5):364–74.
31. Avrahami E, Englender M. Relation between CT axial cross-sectional area of the oropharynx and obstructive sleep apnea syndrome in adults. *AJNR Am J Neuroradiol* 1995;16(1):135–40.
32. Ogawa T, Enciso R, Shintaku WH, et al. Evaluation of cross-section airway configuration of obstructive sleep apnea. *Oral Surg Oral Med Oral Pathol Oral Radiol Endod* 2007;103(1):102–8.
33. Chen NH, Li KK, Li SY, et al. Airway assessment by volumetric computed tomography in snorers and subjects with obstructive sleep apnea in a Far-East Asian population (Chinese). *Laryngoscope* 2002; 112(4):721–6.
34. Barkdull GC, Kohl CA, Patel M, et al. Computed tomography imaging of patients with obstructive sleep apnea. *Laryngoscope* 2008;118:1486–92.